# Optical nonlinearities in multiple quantum wells: Generalized Elliott formula

Domenico Campi and Claudio Coriasso
*CSELT—Centro Studi e Laboratori Telecomunicazioni, Via G. Reiss Romoli 274, 10148 Torino, Italy*
(Received 22 July 1994; revised manuscript received 5 December 1994)

Excitonic nonlinearities due to plasma effects in quantum-well structures under quasistationary excitation can be reproduced by appropriate many-body treatments, which usually require numerical calculations that may become computationally intensive. An alternative approach is based on analytical approximations; however, this has not been examined carefully so far. In this paper we present the analytical calculation of the optical properties of quasi-two-dimensional, type-I semiconductor quantum wells, at varying plasma densities and accounting for one conduction band and two valence subbands. This has been developed based on the two-dimensional version of the Elliott formula and on some analytical approximations already known in part. The obtained analytical results are scalable to a considerable range of constituent materials and of quantum-well thicknesses. These results are compared with the numerical solutions achieved within a more complete many-body approach, based on the Bethe-Salpeter equation, and with experimental results obtained in a pump-probe experiment. The comparison provides general guidelines on the accuracy and on the limitations of the analytical approach applicable to the case of quasi-two-dimensional excitons when multisubband and finite-size effects are included.

## I. INTRODUCTION

Nonlinear optical properties in quasi-two-dimensional electron systems have been studied extensively during the past years, both theoretically and experimentally.[1–24] Almost all experiments in which (light-) intensity-dependent changes of optical properties are measured, or used to obtain optical bistability, are carried out in the photon-energy range of the excitonic absorption peak. These changes are due to the photogeneration of a carrier plasma by the incident radiation. Within this context, the inclusion of many-body effects is thus essential to any calculation of optical properties of quantum wells (QW's), since these dictate in large measure the form of the absorption edge and its evolution with the incident pump power. There have been several investigations concerning many-body theory in semiconductors, in which plasma effects give rise to the large room-temperature nonlinearities in QW's. Actually, compared to the wealth of literature concerning the basic aspects, few simplified expressions in practical structures have been reported so far. Even though some earlier works on nonlinearities in QW's included a few approximate analytical or phenomenological evaluations of many-body effects,[24–30] it is fair to say that, to our knowledge, there has not been any systematic analytical approach to nonlinear optical properties in QW's, although sparse elements can already be found, scattered in the existing literature.

It has been suggested[31–37] that waveguides based on quantum-well materials should display interesting dynamical behavior, that could be analyzed, for example, through equations governing the evolutions of two counterpropagating fields, coupled with one carrier density equation.[38,39] However, one crucial aspect in solving dynamical equations describing optical nonlinearities is the proper treatment of terms describing the field-matter interaction. In principle, this would require a complete description of many-body effects at each computational step and at each wavelength. Most of these calculations are done numerically using algorithms that are not particularly simple and require recursive or iterative approaches that become computationally intensive. In practice, one might use a phenomenological expression, with parameters derived either from theory or experiment: even this is not completely satisfactory, since it would involve interpolations that might become particularly dangerous in treating nonlinear problems. In this respect, a simple formulation of the optical properties, accounting analytically for plasma effects under quasistationary excitation, might be useful.

This paper proposes a systematic formulation of the nonlinear optical properties of QW structures, providing a generalized form of the two-dimensional Eliott formula, and enlightening strengths and weaknesses in the approach. The relevant equations are derived as physically interpretable analytical approximations of more complete many-body treatments that can be found in the literature.[2] This model is tested against numerical calculations in a more complete many-body picture, and against experimental results. Both numerical and experimental results have been obtained as part of this work. Wherever its implementation is regarded as convenient, this method eliminates the use of computationally intensive numerical solutions which previous techniques employed,[39] since even differentiation and integration and other potentially time-consuming operators are avoided in the final expressions.

The outline of the paper is as follows: in Sec. II our generalized expression of the Elliott formula will be provided, and the various terms entering the formula will be described and explained, leaving algebraic details for the appendixes. In Sec. III we will discuss the analytical results, obtained with our formula, and we will compare these results with experimental spectra obtained in a

0163-1829/95/51(16)/10719(10)/$06.00  

pump-probe experiment and with the numerical solution achieved within a more complete many-body approach based on the Bethe-Salpeter equation. A summary and conclusions will be given in Sec. IV.

## II. GENERALIZED ELLIOTT FORMULA

The theoretical foundation of our treatment of the optical response function is the Elliott formula for allowed, direct interband transitions.[40] This has been evaluated both in three (3D) (Ref. 40) and two dimensions (2D),[41] and implies in both cases that the electron-hole correlation produces peaks in the imaginary part of the refractive index $k$, at energies corresponding to the $s$ exciton states $\Psi_n(r)$, with strength $|\Psi_n(r=0)|^2$.

The Elliott formula in the form given in Ref. 41 refers to a rather idealized 2D system. In particular it does not account for any broadening mechanism that causes the excitonic peaks to acquire a finite spectral width, and it does not account for the effects of a finite width of the QW on the binding energy and oscillator strength of the exciton. Further it considers one single subband in either the valence or conduction band.

In our approach we propose a modified version of this formula in order to account for the effects described above, and to include those effects that are relevant to the carrier density dependence of the optical properties in multiple quantum wells (MQW's). Our final expression depends on both energy ($E$) and carrier density ($N$), and refers to a three-subband system, considering one electron subband, one heavy-hole (hh) subband, and one light-hole (lh) subband. It reads

$$k(E,N)=\frac{\hbar c}{2E}\alpha(E,N)=k_{\rm hh}(E,N)+k_{\rm lh}(E,N)\ ,$$

where $\alpha(E,N)$ is the nonlinear absorption coefficient, and where

$$k_j(E,N)=\frac{\hbar c}{2E}\left\{\frac{1}{\pi}\frac{A_{e,j}}{\xi_j}\frac{\frac{\Gamma_j(E_{p,j})}{2}}{\frac{\Gamma_j(E_{p,j})^2}{4}+\left[\frac{E-E_{p,j}}{\xi_j}\right]^2}+f_j A_{c,j}\frac{a_{0,j}/a_j}{1+\theta(E-E_{g,j})\exp\left\{-2\pi\left[\frac{E-E_{g,j}}{Ry_j}\right]^{-1/2}\right\}}\right.$$
$$\left.\times\left\{\frac{1}{2}+\frac{1}{\pi}\arctan\left[\frac{2(E-E_{g,j})}{\Gamma_j(E_{g,j})}\right]\right\}\right\}\ , \tag{1}$$

with $j=$hh and lh.

In this equation $f_j$ is the occupation factor, and $A_{e,j}$ and $A_{c,j}$ are density-dependent transition strengths, while $\Gamma_j$ and $\xi_j$ are an energy-dependent and a density-dependent broadening term, respectively. Here $a_{0,j}=4\pi\varepsilon\hbar^2/q^2 m_0\mu_j$ is the Bohr radius, while $a_j$ is the exciton radius, which becomes $a_{0,j}/2$ in the 2D limit; $m_0$ is the free-electron mass; $q$ is the electron charge; $\varepsilon$ is the background dielectric constant; and $\mu_j=(m_e^{-1}+m_j^{-1})^{-1}$ is the reduced effective mass, with $m_e$ and $m_j$ the electron and hole effective masses. Further, $Ry_j=q^4 m_0\mu_j/2(4\pi)^2\varepsilon^2\hbar^2$ is the Rydberg constant. Finally, $E_{g,j}$ and $E_{p,j}$, respectively, are the renormalized energy gap and the spectral position of the exciton peak.

In our treatment each allowed transition exhibits a 1$s$ exciton peak at its onset and a correlated continuum above the edge. Under general and commonly used assumptions, our model spectra for the extinction coefficient (that is, the imaginary part of the refractive index) consist of two step functions, proportional respectively to the joint density of states for the hh-$e$ and the lh-$e$ transitions. In addition, we have two Lorentzian line shapes for the 1$s$ excitonic resonances.

### A. Continuum contribution

The enhancement of the continuum can be described (both in 2D and 3D) by the so-called Sommerfeld factor, which is a smooth function of momentum (or energy). In our model, Eq. (1), we use a 2D joint density of states, irrespective of the QW thickness, and rescale the absorption coefficient for the continuum of a given transition $j$ using the substitution $a_{0,j}/2\rightarrow a_j$, or, equivalently, we assume an effective Sommerfeld factor to be proportional to $a_{0,j}/a_j$, in order to account for the finite thickness of the QW. We note that a rigorous derivation of this choice could be given in terms of the rescaling theory expounded in our Ref. 42. Thus, for a transition involving subband $j$, the continuum contribution to the extinction coefficient consists, for each subband, of a step function proportional to the joint density of states:

$$k_{j,0}^{\rm cont}=\frac{\hbar c}{2E}A_{c,j}S_j\theta(E-E_{g,j})\ . \tag{2}$$

Here

$$S_j=\frac{a_{0,j}/a_j}{1+\exp\left\{-2\pi\left[\frac{E-E_{g,j}}{Ry_j}\right]^{-1/2}\right\}}$$

represents the Sommerfeld enhancement factor, where we have used the functional energy dependence described in Ref. 24. The step function, Eq. (2), has to be multiplied by an occupation factor $f_j$ and convoluted (see Appendix A) with some appropriate line shape in order to account

for homogeneous and inhomogeneous broadening effects. The line shape, which in this case is a modified Lorentzian form, has been chosen following Haug *et al.*[6] This approach uses an energy-dependent broadening factor which merits some comments: this had been introduced rigorously in Refs. 6, 25, and 43, in order to account for dynamical aspects of broadening, which had previously been studied in Refs. 11, 44, and 45. Based on the literature cited, we use

$$\Gamma_j(E_{g,j})=\frac{2(\Gamma_0+\Gamma_i)}{\exp[-3\beta(E-E_{g,j})]+1}\ , \tag{3}$$

where $\beta=1/kT$, $\Gamma_0$ is an energy broadening parameter which practically accounts for both phonon scattering and any breaking in the translational invariance, and $\Gamma_i$ accounts for unintentional doping in the structure. In the absence of plasmas, most of the deviation from the infinite carrier lifetime is due to sample inhomogeneities, particularly well width fluctuations, and, thus, $\Gamma_0$ and $\Gamma_i$ turn out to be quality-dependent parameters.

### B. Excitonic contribution

In our model, a suitable (analytical) description of the exciton resonance is essential, both for the *e*-hh exciton and the *e*-lh one. To achieve this we use a Lorentzian line shape having an energy-dependent broadening parameter, given by Eq. (3). In addition, we must provide an expression for the oscillator strength of the quasi-2D exciton. A detailed analysis carried out in Ref. 46, which is based on the Elliott formulation of the optical susceptibility[40] and on the work by Shinada and Sugano,[41] relates the exciton oscillator strength for a certain transition to the height of the (correlated) continuum as evaluated at the band edge for the same transition. The two quantities are related through a function expressing the dimensionality of the system,[46] which can vary between 2 and 3. This function is in turn related, in a very simple way, to the binding energy of the exciton,[42] as it can be obtained by solving the quasi-2D electron-hole Schrödinger equation. Using this relationship, the strength of the exciton resonance can be written

$$A_{e,j}=2A_{c,j}Ry_j(-E_{b,j})^2\ , \tag{4}$$

where $E_{b,j}$ is the binding energy of the exciton, expressed in Rydberg units. This equation is valid, in the absence of carriers, for a quasi-2D system, whose dimensionality is between 2 and 3. To proceed further, one has to consider the many-body equation for the exciton in the presence of the plasma: for low plasma densities $N\ll a_0^{-2}$, this can be solved perturbatively by expanding to first order about unperturbed exciton states, thereby obtaining the analytical phase-space filling and exchange corrections to the oscillator strength of the exciton, as illustrated thoroughly in Ref. 47. This evaluates the changes in the oscillator strength Eq. (4) that are due to the filling of states (by bound or unbound particles), which, as a result, become unavailable for the formation of excitons, thereby reducing the overall probability of the resonant creation of excitons. Thus the density-dependent oscillator strength becomes

$$A_{e,j}=\frac{2A_{c,j}Ry_j(-E_{b,j})^2}{1+N/N_{S,j}}$$

where $N_{S,j}=1/3\pi a_j^2$ is the saturation density of a 2D exciton due to a quasithermal plasma made of electrons and holes of type $j$,[47] which we parametrized as previously with $a_{0,j}/2\rightarrow a_j$. The effects discussed here are at the origin of the exciton peak quenching that is currently observed, for instance, in pump-probe experiments.[48–51]

The wave-function renormalization induced by the phase-space filling is the cause of a considerable reduction of the exciton lifetime, and a consequent increase of the broadening of the exciton peak. Following guidelines offered in Ref. 47, this collisional broadening may be viewed as being determined by a density-dependent increase of the exciton radius, causing an enhancement of the (geometrical) cross section for microscopical scattering events in a diluted exciton system. In first perturbative order, this enhancement is proportional to $[1+N/N_s]^2$. A device to incorporate this dependence correctly in the treatment of nonlinear optical properties is given in Appendix B, and it has been introduced by us into Eq. (1).

Consistently with the description given in Appendix B, the exciton contribution to refractive properties can be obtained through

$$n_j^{\rm exc}(E,N)=\frac{\hbar c}{\pi E}\frac{A_{e,j}}{\xi_j}\frac{\dfrac{E_{p,j}-E}{2\xi_j}}{\dfrac{\Gamma_j(E_{p,j})^2}{4}+\left[\dfrac{E-E_{p,j}}{\xi_j}\right]^2}\ . \tag{5}$$

Many of the quantities that have been examined in the present analytical treatment are referred to the exciton radius or to the exciton binding energy. These quantities have been given a rather simple form in Ref. 42, as a result of a variational treatment of the two-body Schrödinger equation describing the exciton in a quasi-2D system

$$E_{b,j}=-\left[\frac{2}{d_j-1}\right]^2,\quad a_j=a_{0,j}\left[\frac{d_j-1}{2}\right],$$

where $d_j$ is the exciton dimensionality, which can be evaluated using the equation introduced in Ref. 52; see Table I.

We may note that the analytical model does not depend on the particular expression we choose for the binding energy; it simply requires a value that can be calculated either analytically or numerically in order to have explicit access to the rescaling of the exposed theory. Transition selection rules, including polarization-dependent effects, are incorporated into the momentum matrix element (see Table I). Within this picture, the coupling between the two valence subbands takes place through filling and screening properties, and through self-energy corrections (see Appendixes C, D, and E for explicit derivations). Refractive changes related to excitonic contributions can be obtained from Eq. (5), evaluated for both the heavy- and light-hole transitions. The continu-

TABLE I. Parameters used in the calculation of optical properties of structure No. 191. The masses are given in units of the free-electron mass and $\varepsilon_0$ represents the vacuum permittivity. The conduction-band to valence-band offset ratio used in the calculations is 40/60. The masses along the growth direction have been used, as these are recognized to give the best representation of the complicated behavior at the center of the Brillouin zone (Ref. 2).

| | |
|---|---|
| Well width | $L_W=9.4$ nm |
| Barrier width | $L_B=8.0$ nm |
| Number of wells | $N_W=66$ |
| Electronic level | $L_e=0.044$ eV |
| Heavy-hole level | $L_{hh}=0.008$ eV |
| Light-hole level | $L_{lh}=0.037$ eV |
| Heavy-hole band gap | $E_{g,hh}^W=0.761$ eV |
| Light-hole band gap | $E_{g,lh}^W=0.745$ eV |
| Electron effective mass | $m_e$ $(L_e)=0.043$ |
| Heavy-hole effective mass | $m_{hh}$ $(L_{hh})=0.423$ |
| Light-hole effective mass | $m_{lh}$ $(L_{lh})=0.056$ |
| Heavy-hole exciton dimensionality | $d_{hh}=2.29$ |
| Light-hole exciton dimensionality | $d_{lh}=2.21$ |
| Lorentzian width (doping contribution) | $\Gamma_i=5$ meV |
| Lorentzian width (other contributions) | $\Gamma_0=12.5$ meV |
| Background dielectric constant | $\varepsilon=12.74\varepsilon_0$ |
| Band gap refractive index | $n_g=3.5$ |
| Momentum matrix element (light polarized in the plane of the QW's) | $P_j=2.35\times\begin{cases}0.75(\text{hh})\\0.25(\text{lh})\end{cases}$ eV |

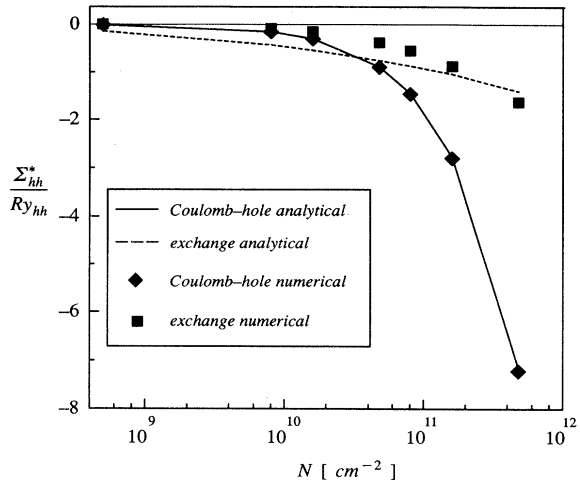


FIG. 1. Self-energy correction terms to the heavy-hole energy-gap vs the photogenerated plasma density $N$, calculated for a MQW system in the analytical approach. The Coulomb-hole and exchange (solid and dashed) curves calculated for vanishing momentum wave vector in the fully numerical approach are also comparatively shown.

um contribution to refractive changes could be calculated by performing a Kramers-Kronig transformation of the relevant term in the extinction coefficient (the second term in parentheses in Eq. (1)]. This was found to be small in the density range discussed here and for energies lower than the band gap, as will be discussed further in Sec. III. Thus, if one is interested in the spectral region located below the band gap, where waveguided propagation is usually studied, one option is to neglect continuum contributions to refractive changes.

## III. DISCUSSION

Although quite elaborate and rigorous many-body treatments are known, we prefer to base our considerations on a computational scheme, introduced in Ref. 2. This scheme includes (1) the effective-mass approximation, (2) the random-phase approximation (RPA) and the plasmon-pole approximation for the longitudinal dielectric constant, (3) the quasistatic approximation of the dielectric screening, and (4) the solution of the Bethe-Salpeter equation for the two-particle Green's function using the ladder approximation. Its original formulation treated QW's with only one conduction and one valence subband in the purely 2D limit, but suitable extensions have been provided that allow the treatment of multisubband QW's of finite thicknesses.[8–11,53,54] This theoretical picture is relatively simple and has been implemented by several workers, since it is able to reproduce many central features that are observed in nonlinear optical experiments performed on QW structures. As such, it can provide a good starting point to derive an analytical formulation of plasma effects on optical properties, as we have shown. In addition, its computational outcomes can be used to evaluate the approximations adopted, as is shown below. Both analytical and numerical calculations are implemented here in some test cases corresponding to real structures, which we have addressed experimentally as part of this work using a stationary pump-probe experiment. In Fig. 1 we exhibit the Coulomb-hole and the exchange self-energy corrections for the heavy-hole transitions, calculated as in Appendix C. In the same figure the self-energy corrections calculated numerically in the quasistatic approach described in Ref. 11 are shown comparatively. The calculations are performed at vanishing momentum wave vector.

The experimental technique adopted is similar to that illustrated in Ref. 55, where an intense pump beam from a Nd:YAG (yttrium aluminum garnet) laser is used to generate a plasma inside the sample, and a broadband continuum is used as a weak probe to measure the transmission through the structure at varying wavelength and pump power.

A graphical representation of both computational and experimental results helps in the comparison. In Fig. 2 we exhibit the absorption coefficient at varying plasma densities, as a function of the photon energy of the probe beam. In particular, in Fig. 2(a) we show the results of the pump-probe experiment carried out on a $66\times(L_W=9.4/L_B=8.0$ nm) $In_xGa_{1-x}As/InP$ MQW sample at 300 K, while Figs. 2(b) and 2(c) represent fully numerical and analytical solutions, respectively. The parameter values adopted in the calculations are summa-

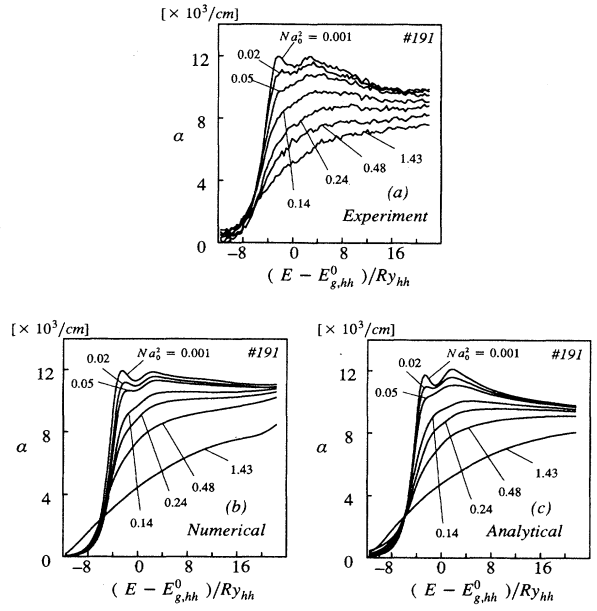


FIG. 2. Absorption spectra of a MQW system containing 66 periods ($L_W = 9.4$ nm and $L_B = 8.0$ nm), for various plasma densities $Na_0^2$ at room temperature: (a) is relevant to the pump-probe experiment on sample No. 191; (b) refers to the fully numerical solution based on the many-body theory; (c) is obtained using the analytical approach. The linear ($Na_0^2 = 0.001$) spectrum shows two exciton peaks, corresponding to the heavy-hole and light-hole exciton, respectively. Spectra refer to the TE polarization of the probe beam.

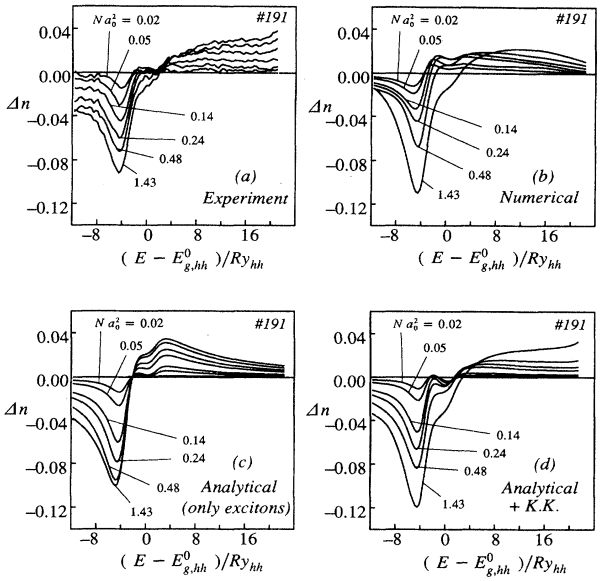


FIG. 3. Refractive changes with respect to the linear spectrum and for different plasma densities: (a) experimental data obtained by Kramers-Kronig transformation of the experimental absorptive changes; (b) theoretical curves obtained in the fully numerical approach based on the many-body theory; (c) theoretical curves obtained using the analytical approach (only the excitonic contributions have been presented here); (d) theoretical curves obtained using the analytical approach by adding the excitonic refractive variations to the Kramers-Kronig transform of analytically calculated absorptive changes relevant to the continuum. The Kramers-Kronig transform has been calculated numerically. Both experimental and calculated spectra refer to the TE polarization of a probe beam.

rized in Table I. Concerning the quality-dependent parameter $\Gamma_0$, we preferred to estimate the relevant value from the linear absorption spectrum obtained in the experiment, although some form of theoretical estimation would be possible.[29,56] In the experimental curves, the plasma densities were related to the power densities according to a 2.5-ns radiative decay time constant.[55]

A plot of the refractive changes is shown in Fig. 3. The experimental data [Fig. 3(a)] have been obtained from the Kramers-Kronig transform of the absorption difference data. Figure 3(b) shows the fully numerical results; Fig. 3(c) shows the analytical results accounting for the excitonic contributions only, while in Fig. 3(d) the analytical results relevant to the excitonic contributions have been added to the numerical Kramers-Kronig transform of the continuum contribution, evaluated analytically. From the comparison of Figs. 3(c) and 3(d) we see that, within the plasma-density range examined here and for energies in the transparence region, $\Delta n$ changes only insignificantly with the addition of the continuum contributions.

In Fig. 4, we report the comparison between analytical and numerical nonlinear absorption coefficient calculations, relative to further $In_xGa_{1-x}As/InP$ MQW samples. The first structure (No. 107) is a $60\times(L_W = 7.7$ nm$/L_B = 7.0$ nm) MQW, while the second one (No. 401) is a $66\times(L_W = 5.5$ nm$/L_B = 7.0$ nm) MQW.

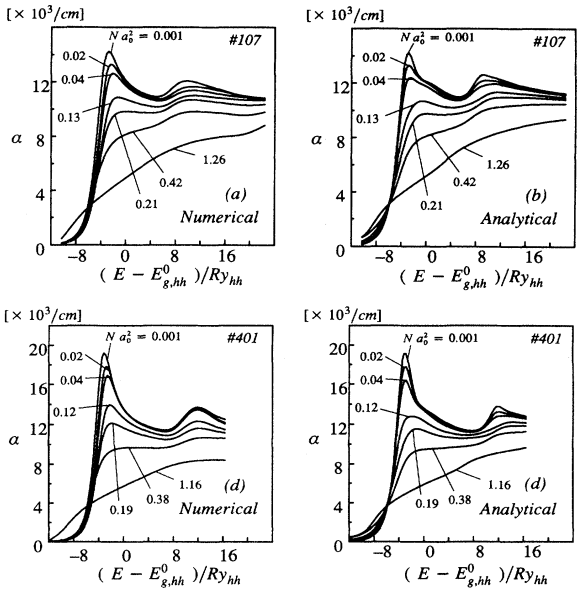


FIG. 4. Absorption spectra of two MQW systems. Numerical and analytical results for sample No. 107, containing 60 periods ($L_W = 7.7$ nm and $L_B = 7.0$ nm), are shown in (a) and (b), respectively, while numerical and analytical results for sample No. 401, containing 66 periods ($L_W = 5.5$ nm and $L_B = 7.0$ nm), are shown in (c) and (d), respectively.

In what follows we present some comments on the results and limitations of the analytical model presented. First of all, our analytical treatment incorporates the same limitations of the more complete many-body picture from which it was derived. Actually, this latter approach has been criticized in the literature,[12,23] and it is known to yield self-energy corrections that are overestimated in the high-density regime. In addition, both numerical and analytical approaches assume that the electron-hole plasma be thermalized into a quasiequilibrium situation.

One further limitation of the current analytical model is that some approximations we have adopted are used outside their natural range of validity. The reason is that, in order to be of some usefulness, the model has to consider a relatively broad range of values of $N$, while the quantities appearing in the model are often evaluated either in a low-density limit or in a high-density approximation, depending on our ability to find some analytical expression. For example, the exchange self-energy has been evaluated by us in a degenerate limit, and, as we note, the RPA is in itself a high-density approximation. Fortunately, however, in this case the behavior in the low-density limit is not quantitatively important, since the relevant self-energy corrections would be very small anyway (of order one Ry or less), and the absolute error is consequently small, even if the relative error can be very high. In addition to that, we note that some density-dependent quantities have been evaluated perturbatively in the limit $N/N_s \ll 1$, while these are used in the full density regime. In particular, the density-dependent broadening mechanism, the oscillator strength, and even the location of the exciton peaks have been treated in this way. However, the exciton peak tends to broaden and bleach very rapidly already at small density values: again, errors in quantities that determine a spectral structure which is very small and broad tend to become unimportant. These considerations may help to explain the true nature of the relatively good match between the analytical model and the many-body treatment, which we regard as somewhat fortuitous, although systematic.

Our comparison suggests further that the small blueshift of the exciton peak observed at very low densities in both the numerical treatment and experiment is not correctly represented. Typically, this plays a negligible role in the behavior at the exciton peak and at room temperature, but should be accounted for in any picture purporting to describe the behavior at energies below the exciton peak. In Ref. 47, an evaluation of a blueshift correction to the exciton binding energy was proposed, but this is found by us to be largely underestimated at low densities, and largely overestimated at high plasma density, when compared either to the numerical or to the experimental spectra. As a result it is not advisable to introduce this term into the model.

## IV. SUMMARY AND CONCLUSIONS

In summary, the approach investigated here provides a physically interpretable approximation adequate for obtaining the correct trends of optical spectra in the presence of thermalized plasmas. It is generally more quantitative and accurate than the purely 2D and one-subband numerical approaches, but it is unable to reproduce details (especially in the energy region below the exciton peak) that in some application may play a role, and that can be correctly predicted using more complete numerical calculations. The method does not involve any fitting or interpolation parameter and its primary computational advantage is that CPU times are reduced by a factor at least $10^3$ with respect to the numerical approach. Besides this, the analytical approach proposed here possesses some potential to predict experimental conditions that may be of interest for specific applications, and trends and limiting cases that may not immediately be apparent in the more rigorous but more involved theory. With minor modifications the model could be used to obtain the optical response in the presence of unipolar plasmas,[21,57] like in barrier reservoir and QW electron transfer (or BRAQWET) structures.[58]

One natural extension to this work would be to incorporate the analytical model into a dynamical modeling of waveguide behavior, of the kind exposed in Refs. 38 and 39.

## APPENDIX A: BROADENING EFFECTS ON THE CONTINUUM CONTRIBUTION

Broadening effects are introduced into the continuum contribution of the extinction coefficient using a convolution with a modified Lorentzian line shape.[6] In order to make the convolution integral feasible analytically, we adopt the approximation of factoring both the occupation factor and a weak energy dependence relevant to the Sommerfeld enhancement out of the convolution integral: this approximation is justified since the typical broadening of the occupation factor at room temperature is much larger than the broadening of the line shape in the integrand, with a similar justification holding for the Sommerfeld enhancement. The convolution can then be obtained analytically integrating by parts:

$$k_j^{\mathrm{cont}}(E,N)=\frac{1}{\pi}\int_0^{\infty}dE'\frac{\Gamma_j(E')/2}{\Gamma_j(E')^2/4+(E-E')^2}f_j k_{j,0}^{\mathrm{cont}}(E')$$

$$\simeq\frac{\hbar c}{2E}f_j A_{c,j}\frac{a_{0,j}/a_j}{1+\theta(E-E_{g,j})\exp\left\{-2\pi\left[\frac{E-E_{g,j}}{Ry_j}\right]^{-1/2}\right\}}\left\{\frac{1}{2}+\frac{1}{\pi}\arctan\left[\frac{2(E-E_{g,j})}{\Gamma_j(E_{g,j})}\right]\right\},$$

where $A_{c,j}=2(\alpha\mu_j P_j/n_g m_e L_W E^0_{g,j})$, $k^{\rm cont}_{j,0}$ is given in Eq. (2), and the occupation factor $f_j$ is discussed in Appendix E.

Here $P_j$ represents the squared momentum matrix element for the transition $j$-$e$, which has been considered constant in energy since our interest is focused on a limited spectral range and since its energy dependence is weak. Further, $n_g$ is the refractive index of the structure at the band edge, $L_W$ is the QW thickness, and $\alpha$ is the fine-structure constant. The transition energy at zero plasma concentration is defined $E^0_{g,j}=E^W_{g,j}+L_e+L_j$, where $L_e$ and $L_j$ are the quantized levels of the conduction- and valence-band profiles, pertaining to the heavy-hole ($j$=hh) or light-hole ($j$=lh) subbands, while $E^W_{g,j}$ is the energy gap of the well material.

## APPENDIX B: EXCITONIC CONTRIBUTION

The appearance of density dependence in exciton broadening is particularly important in view of a correct description of the resonance quenching.[23] However, it is worth noting that this picture is not deemed to apply to the inhomogeneous broadening terms [$\Gamma_0$ in Eq. (3)] accounting, e.g., for well width fluctuations and other inhomogeneities which tend to reduce the lifetime of the exciton constituents, inducing a finite decay time of single-particle states characterized by a well-defined momentum. In some sense, these factors limit the lifetime of the exciton by limiting the lifetime of the states occupied by the constituents, and do contribute to the exciton linewidth, but do not display any density dependence. All that taken into account, we can finally express the lineshape of the exciton peak, accounting for plasma-related reflects on the broadening:

$$k^{\rm exc}_j(E,N)=\frac{\hbar c}{2\pi E}\frac{A_{e,j}}{\xi_j}\frac{\frac{\Gamma_j(E_{p,j})}{2}}{\frac{\Gamma_j(E_{p,j})^2}{4}+\left[\frac{E-E_{p,j}}{\xi_j}\right]^2},$$

where

$$\Gamma_j(E_{p,j})=\frac{2(\Gamma_0+\Gamma_i)}{\exp[-3\beta(E-E_{p,j})/\xi_j]+1}$$

and

$$\xi_j=\frac{\Gamma_0+\Gamma_i(1+N/N_{S,j})^2}{\Gamma_0+\Gamma_i}.$$

The location $E_{p,j}$ of the exciton resonance on the energy axis is determined by the binding energy and by the energy gap; the binding energy undergoes a vertex correction, due to the phase-space filling effects. This correction can be predicted by a perturbation approach, and, in first order, it is found to have two contributions that cancel exactly the exchange and Coulomb-hole self-energy corrections to the energy gap.[3] Thus, at least for very low-density values, the energy location of the exciton peak does not show any dependence on $N$, and is locked to the zero-density position $E_{p,j}=E^0_{g,j}+E_{b,j}Ry_j$. This is verified to a very good approximation both in the numerical solution of the many-body problem and in the experimental spectra. However, recent experimental spectra show that at relatively high densities, but still with the exciton not entirely bleached, the exciton peak can display either a redshift or a slight blueshift (see Fig. 2 in Ref. 59). Actually, only theories including full dynamical screening and, possibly, corrections beyond the random-phase approximation may give a description of the carrier dependence of the exciton peak which is generally accurate.

## APPENDIX C: PLASMA SCREENING

A key feature in the calculation of the population effects in semiconductors is the value of the quasi-Fermi levels for electrons and holes. If the subbands to be considered can be reduced to one, as it is often the case for the conduction band, the quasi-Fermi level $E^c_F$ can be given exactly:

$$E^c_F=L_e+\frac{1}{\beta}\ln\left[\exp\left[\frac{\pi N\beta\hbar^2}{m_0 m_e}\right]-1\right],$$

where $L_e$ is the quantized electron level.

An exact expression cannot be obtained for the case of more than one subband. However, considering only two valence subbands, and if the population in one of the two valence subbands (the lh subband) can be assumed to be small with respect to that in the other one (the hh subband), one can obtain a very accurate estimate of the quasi-Fermi level in the valence band $E^v_F$ using

$$E^v_F=L_{\rm hh}+\frac{1}{\beta}\ln\{b[1+a(b\{1+a[b(1+t)^{-r}-1]\}^{-r}-1)]^{-r}-1\}, \quad \text{(C1)}$$

where $a=\exp[\beta(L_{\rm hh}-L_{\rm lh})]$, $b=\exp(\pi N\beta\hbar^2/m_0 m_{\rm hh})$, $r=m_{\rm lh}/m_{\rm hh}$, $t=a(b-1)$, and $L_{\rm hh}$ and $L_{\rm lh}$ are the quantized heavy- and light-hole levels, respectively.

This has been obtained by inverting the population equation by successive approximations, and it can be regarded as a correct evaluation in all cases in which the masses in the two valence subbands differ appreciably. In the cases examined within this paper, we found that the agreement between the formula Eq. (C1) and the numerical inversion of the population equation[60] is better than 1%. The same good match was found in all practical cases examined so far, although a word of caution concerning mostly tensile-strained materials is in order. In specific cases, the validity of Eq. (C1) should be tested in advance, along with the validity of the effective-mass approximation.

In a typical nonlinear experiment, a strong pump beam photogenerates a plasma formed by electrons and holes, which is here assumed to reach thermal quasiequilibrium instantaneously in the time scale which characterizes the

experiments we intend to model. A weak probe, often tunable in energy, resonantly excites pairs in the material, eventually forming excitons, or unbound (but still correlated) electron-hole pairs. The Coulomb interaction between the pairs formed by the probe is screened: at high temperature, the screening is governed by free carriers and can be described by the random-phase approximation (RPA).[61–63] In coordinate space, the screened Coulomb potential can be approximately described by the Yukawa potential, both in the two- (2D) and three-dimensional (3D) limits:[61] $V_s(r)=V(r)\exp(-\kappa r)$, where $\kappa$ is a screening vector (or inverse screening length) defined as in Ref. 61, and discussed in our Ref. 11 for a multisubband system. In order to evaluate this analytically, we neglect, to a good approximation, the contribution of the light holes, obtaining $\kappa\sim\kappa_e+\kappa_{\rm hh}$, where

$$\kappa_e=2\frac{m_0 m_e q^2}{4\pi\varepsilon\hbar^2}\left[1-\exp\left[-\frac{\pi N\beta\hbar^2}{m_0 m_e}\right]\right],$$

$$\kappa_{\rm hh}=2\frac{m_0 m_{\rm hh} q^2}{4\pi\varepsilon\hbar^2}\left[1-\exp\left[-\frac{\pi N\beta\hbar^2}{m_0 m_{\rm hh}}\right]\right].$$

## APPENDIX D: SELF-ENERGY CORRECTIONS

Knowing the screened Coulomb interaction, one can readily determine the changes of the single-particle energies, within the frame of the RPA, and with the further, simplifying assumptions of the quasistatic plasmon-pole description.[2] This evaluates the band-gap renormalization; that is, the energy that is gained by the particles by correlating their motions. This is split into two contributions, the screened-exchange (proper) self-energy $\Sigma^{*\rm exc}$, and the Coulomb-hole or correlation (proper) self-energy $\Sigma^{*\rm Ch}$. A simple approximation for the exchange self-energy term is obtained in the literature,[25] by considering momentum transfers at the Fermi surface only. Here we preferred to adopt a different approximation which can be obtained by taking the zero-temperature expression of the Fermi distribution in the integral which yields the exchange self-energy term, since this guarantees a better reproduction of the more rigorous exchange correction evaluated numerically. This yields

$$\Sigma_j^{*\rm exc}=-\frac{\hbar^2}{2a_{0,j}m_0\mu_j}\left[\kappa\ln\left[\frac{\kappa}{k_F+\kappa}\right]+k_F\right], \quad \text{(D1)}$$

where $k_F=\sqrt{2\pi N}$ is the Fermi impulse.

For the Coulomb-hole term, we adopt the approximation described in Ref. 25,

$$\Sigma_j^{*\rm Ch}=-\frac{\hbar^2}{2a_{0,j}m_0\mu_j}\kappa . \quad \text{(D2)}$$

We note that this is a very simple approximation, which neglects a term of order $q^4$ (with $q$ being the momentum) in the expression of the effective plasmon frequency (see Ref. 61, p. 143). A less approximate expression, accounting for the terms $O(q^4)$ is given in Ref. 64. This involves the introduction of an integration cutoff in order to avoid a logarithmic divergence, whose definition, although conceptually correct, is somewhat arbitrary as discussed in Ref. 5. However, in the range of carrier densities investigated by us, we generally found Eq. (D2) in the above to give results that are closer to our experimental findings than the equation provided in Ref. 64. This is especially important because the Coulomb-hole correction is the dominant one in the density range addressed by us. In view of this we preferred to adopt Eq. (D2) in the above rather than Eq. (2.11) of Ref. 64.

We note further that we neglected a weak momentum dependence, approximating the exchange self-energy corrections as rigid band shifts.[5] The terms in Eqs. (D1) and (D2) with $j=$hh, refer to the renormalization of the optical threshold for the excitation of pairs formed by electrons and heavy holes, due to the existence of a plasma occupying electron states, or pairs formed by elecrons and heavy holes, due to the existence of a plasma occupying hole states. Thus

$$\Sigma_{\rm hh}^{*}=2\Sigma_{\rm hh}^{*\rm Ch}+2\Sigma_{\rm hh}^{*\rm exc}$$

where the factors 2 account for the fact that electrons and holes in the plasma yield equivalent corrections.

In our description similar terms, with $j=$lh, also exist for the renormalization of pairs formed by electrons and light holes. However, we note that, since the plasma is assumed to be thermalized, the holes in the plasma would occupy mostly heavy-hole states, displaying no exchange interaction with light-hole constituents of electron–light-hole pairs generated by the probe beam. Thus, the corresponding exchange self-energy term is considered negligibly small. On the contrary, Coulomb corrections hold independently of subband occupation. All this taken into account, we have

$$\Sigma_{\rm lh}^{*}=2\Sigma_{\rm lh}^{*\rm Ch}+\Sigma_{\rm lh}^{*\rm exc} .$$

Thus, in the presence of a plasma, the minimum energy required for a probe photon to resonantly excite pairs in the material is either $E_{g,\rm hh}=E_{g,\rm hh}^0+\Sigma_{\rm hh}^{*}$ or $E_{g,\rm lh}=E_{g,\rm lh}^0+\Sigma_{\rm lh}^{*}$, depending on the kind of pairs that are formed by the probe beam.

The self-energy corrections in the above are analytical approximations of more rigorous calculations that were originally formulated in the strictly 2D limit. In general, we can expect a dependence of the quantum-mechanical and, consequently, the optical properties of a QW on the thickness of the QW material. In particular, this holds true for the exchange self-energy correction in the above, and can be accounted for by using the parametrization $a_{0,j}/2\rightarrow a_j$: this formally replaces the 2D limit of the exciton radius with its actual value, which is a function of the QW thickness and is defined to be $a_{0,j}/2\le a_j\le a_{0,j}$, where the Bohr radius $a_{0,j}$ is the exciton radius expected in 3D; thus

$$\Sigma_j^{*\rm exc}=-\frac{\hbar^2}{4a_j m_0\mu_j}\left[k_F+\kappa\ln\left[\frac{\kappa}{k_F+\kappa}\right]\right].$$

The origin of the changes in the self-energy is due to the fact that we would have to adopt a three-dimensional form for the Coulomb potential, instead of a purely 2D one, as we do in our numerical calculations. In fact, the

exchange self-energies in 2D and 3D have different expressions. However, the 2D term (evaluated in the high-density limit) can be made equal to its 3D analog with the changes $a_{0,j}/2 \rightarrow a_{0,j}$, and $\sqrt{N_{2D}} \rightarrow \sqrt[3]{N_{3D}}$, thereby justifying the parametrization (this holds true if a 4% difference in the multiplying constant is neglected). On the contrary, the Coulomb-hole self-energy has the same functional form in 2D and 3D within the approximation adopted by us (see Ref. 61, p. 143). Thus the difference in values between 2D and 3D would depend only on the band-filling properties, and the relevant expression should not be rescaled as long as one uses the same form for the density of state, as is so in our case. The theoretical and experimental foundations of the parametrization introduced here are exposed in a paper by Weber *et al.*,[65] where it is demonstrated that it is generally possible to use 2D theory to describe QW's, under the condition that effective parameters are used for the natural units. In this respect, the exciton radius and its binding energy provide ideal means to scale the theory from one material to another,[27] and from one material thickness to another.

## APPENDIX E: DISTRIBUTION FUNCTIONS

In principle, the task of computing the electromagnetic response of a multisubband system would involve a self-consistent procedure, since both the quasi-Fermi levels and the quantized-level energies are renormalized by plasma effects under excitation, and each subband in the valence band is renormalized by a quantity which is generally different from the shift of the quasichemical potential in the valence band.[11,53] However, we know that various contributions to the renormalization of the valence-band quasi-Fermi level are weighted by the population of the subbands. In practice, thus, we can make the assumption that the quasi-Fermi level in the valence band renormalizes like the heavy-hole subband, which is the most populated one. Under this assumption all quasi-Fermi distribution functions can be given analytical expressions

$$f_{c,j}=[1+\exp(\beta\Delta E_{c,j})]^{-1} ,$$

$$f_{v,j}=[1+\exp(-\beta\Delta E_{v,j})]^{-1} ,$$

$$\Delta E_{c,j}=L_e+\Sigma^*_{e,j}+\frac{\mu_j}{m_e}(E-E_{g,j})-(E^c_F+\Sigma^*_{e,\mathrm{hh}}) ,$$

$$\Delta E_{v,j}=L_j+\Sigma^*_{h,j}+\frac{\mu_j}{m_j}(E-E_{g,j})-(E^v_F+\Sigma^*_{h,\mathrm{hh}}) ,$$

$$\Sigma^*_{e,\mathrm{hh}}=\Sigma^*_{h,\mathrm{hh}}=\Sigma^{*\mathrm{exc}}_{\mathrm{hh}}+\Sigma^{*\mathrm{Ch}}_{\mathrm{hh}} ,$$

$$\Sigma^*_{e,\mathrm{lh}}=\Sigma^{*\mathrm{exc}}_{\mathrm{lh}}+\Sigma^{*\mathrm{Ch}}_{\mathrm{lh}} ,$$

$$\Sigma^*_{h,\mathrm{lh}}=\Sigma^{*\mathrm{Ch}}_{\mathrm{lh}} ,$$

$$f_j=f_{v,j}-f_{c,j} ,$$

where $j=$hh and lh, and the effective-mass approximation has been used for the energy-momentum dispersion.


[1] S. Schmitt-Rink, C. Ell, S. W. Koch, H. E. Schmidt, and H. Haug, Solid State Commun. **52**, 123 (1984).
[2] S. Schmitt-Rink, C. Ell, and H. Haug, Phys. Rev. B **33**, 1183 (1986).
[3] S. Schmitt-Rink, D. S. Chemla, and D. A. B. Miller, Adv. Phys. **38**, 89 (1989).
[4] S. Schmitt-Rink and C. Ell, J. Lumin. **30**, 585 (1985).
[5] H. Haug and S. Schmitt-Rink, J. Opt. Soc. Am. B **2**, 1135 (1985).
[6] H. Haug, J. Liebler, R. Leonelli, A. Manar, and J. B. Grun, Phys. Rev. B **38**, 10 903 (1988).
[7] C. Ell, H. Haug, and S. W. Koch, Opt. Lett. **14**, 356 (1989).
[8] G. D. Sanders and Yia-Chung Chang, Phys. Rev. B **32**, 551 (1985).
[9] Yia-Chung Chang and G. D. Sanders, Phys. Rev. B **32**, 5521 (1985).
[10] Shun-Lien Chuang, S. Schmitt-Rink, D. A. B. Miller, and D. S. Chemla, Phys. Rev. B **43**, 1500 (1991).
[11] D. Campi, P. J. Bradley, R. Calvani, and R. Caponi, IEEE J. Quantum Electron. **QE-29**, 1144 (1993).
[12] S. Das Sarma, R. Jalabert, and S.-R. Eric Yang, Phys. Rev. B **39**, 5516 (1989).
[13] I. K. Marmorkos and S. Das Sarma, Phys. Rev. B **44**, 3451 (1991).
[14] S. Das Sarma and I. K. Marmorkos, Phys. Rev. B **47**, 16 343 (1993).
[15] G. R. Olbright, W. S. Fu, and J. F. Klem, Phys. Rev. B **44**, 3043 (1991).
[16] R. Binder, I. Galbraith, and S. W. Koch, Phys. Rev. B **44**, 3031 (1991).
[17] K. H. Schlaad, C. Weber, J. Cunningham, C. V. Hoof, G. Borghs, G. Weimann, W. Schlapp, H. Nickel, and C. Klingshirn, Phys. Rev. B **43**, 4268 (1991).
[18] D. Huang, Jen-Inn Chyi, and H. Morkoç, Phys. Rev. B **42**, 5147 (1990).
[19] G. D. Mahan and L. E. Oliveira, Phys. Rev. B **44**, 3150 (1991).
[20] I. Galbraith, Phys. Rev. B **48**, 5105 (1993).
[21] R. Cingolani, W. Stolz, and K. Ploog, Phys. Rev. B **40**, 2950 (1989).
[22] R. Cingolani, H. Kalt, and K. Ploog, Phys. Rev. B **42**, 7655 (1990).
[23] D. R. Wake, H. W. Yoon, J. P. Wolfe, and H. Morkoç, Phys. Rev. B **46**, 13 452 (1992).
[24] D. S. Chemla and D. A. B. Miller, J. Opt. Soc. Am. B **2**, 1155 (1985).
[25] C. Ell, R. Blank, S. Benner, and H. Haug, J. Opt. Soc. Am. B **6**, 2006 (1989).
[26] G. Tränkle, H. Leier, A. Forchel, H. Haug, C. Ell, and G. Weimann, Phys. Rev. Lett. **58**, 419 (1987).
[27] G. Tränkle, E. Lach, A. Forchel, F. Scholz, C. Ell, H. Haugh, G. Weimann, G. Griffiths, H. Kroemer, and S. Subanna, Phys. Rev. B **36**, 6712 (1987).
[28] D. A. Kleinman and R. C. Miller, Phys. Rev. B **32**, 2266 (1985).
[29] P. J. Stevens, M. Whitehead, G. Parry, and K. Woodbridge, IEEE J. Quantum Electron. **QE-24**, 2007 (1988).
[30] D. Campi, in *Materials for Photonic Devices*, edited by A. D'Andrea, A. Lapiccirella, G. Marletta, and S. Viticoli

(World Scientific, Singapore, 1991).
[31]P. LiKamWa, A. Miller, C. B. Park, J. S. Roberts, and P. N. Robson, Appl. Phys. Lett. **57**, 1846 (1990).
[32]P. LiKamWa, P. N. Robson, J. P. R. David, G. Hill, P. Mistry, M. A. Pate, and J. S. Roberts, Electron. Lett. **22**, 1129 (1986).
[33]L. Thylen, E. M. Wright, and G. I. Stegeman, J. Opt. Soc. Am. B **5**, 467 (1988).
[34]E. Caglioti, S. Trillo, S. Wabnitz, and G. I. Stegeman, J. Opt. Soc. Am. B **5**, 472 (1988).
[35]G. Assanto and G. I. Stegeman, J. Appl. Phys. **67**, 1188 (1990).
[36]M. Cada, F. Vasey, J. M. Stauffer, and F. K. Reinhart, Appl. Phys. Lett. **59**, 2366 (1991).
[37]C. Cacciatore, D. Campi, C. Coriasso, G. Meneghini, and C. Rigo, Electron. Lett. **28**, 1624 (1992).
[38]G. P. Bava and L. A. Lugiato, Opt. Commun. **78**, 195 (1990).
[39]G. P. Bava, F. Castelli, P. Debernardi, and L. A. Lugiato, Phys. Rev. B **45**, 5180 (1992).
[40]R. J. Elliott, Phys. Rev. **108**, 1384 (1957).
[41]M. Shinada and S. Sugano, J. Phys. Soc. Jpn. **21**, 1936 (1966).
[42]D. Campi and C. Villavecchia, IEEE J. Quantum Electron. **QE-28**, 1765 (1992). After the publication of this paper, the authors discovered a few misprints. For example $\rho$ and $\rho'$ are missing in Eqs. (8) and (9). However, the results are unaffected by this undesirable occurrence.
[43]H. Haug, L. Banyai, C. Ell, and T. Wicht, Proc. SPIE **1280**, 2 (1990).
[44]P. T. Landsberg, Phys. Status Solidi **15**, 623 (1966).
[45]R. W. Martin and H. L. Stormer, Solid State Commun. **22**, 523 (1977).
[46]P. C. Klipstein and N. Apsley, J. Phys. C **19**, 6461 (1986).
[47]S. Schmitt-Rink, D. S. Chemla, and D. A. B. Miller, Phys. Rev. B **32**, 6601 (1985).
[48]A. M. Fox, A. C. Maciel, M. G. Shorthose, J. F. Ryan, M. D. Scott, J. I. Davies, and J. R. Riffat, Appl. Phys. Lett. **51**, 30 (1987).
[49]D. Campi, C. Coriasso, C. Cacciatore, and H. C. Neitezert, Proc. SPIE **2150**, 72 (1994).
[50]M. A. Fisher, J. Appl. Phys. **67**, 543 (1990).
[51]P. J. Bradley, R. Calvani, D. Campi, R. Caponi, and G. Morello (unpublished).
[52]H. Mathieu, P. Lefebvre, and P. Christol, Phys. Rev. B **46**, 4092 (1992).
[53]M. F. Pereira, S. W. Koch, and W. W. Chow, J. Opt. Soc. Am. B **10**, 765 (1993).
[54]M. F. Pereira, R. Binder, and S. W. Koch, Appl. Phys. Lett. **63**, 279 (1994).
[55]P. J. Bradley, R. Calvani, D. Campi, R. Caponi, and F. Genova, Semicond. Sci. Technol. **7**, 552 (1992).
[56]D. Campi, C. Cacciatore, C. Coriasso, C. Villavecchia, and C. Alibert, Proc. SPIE **1280**, 115 (1990).
[57]C. Tombling, M. M. Stallard, and J. S. Roberts, Semicond. Sci. Technol. **5**, 502 (1990).
[58]J. E. Zucker, M. Wegener, K. L. Jones, T. Y. Chang, N. Sauer, and D. S. Chemla, Appl. Phys. Lett. **56**, 1951 (1990).
[59]R. Jin, K. Okada, G. Khitrova, H. M. Gibbs, M. Pereira, S. W. Koch, and N. Peyghambarian, Appl. Phys. Lett. **61**, 1745 (1992).
[60]See, for example, Eq. (100) in C. Weisbuch and B. Vinter, *Quantum Semiconductor Structures* (Academic, New York, 1991), p. 177.
[61]For a general introduction to the many-body theory of excited semiconductors, see H. Haug and S. Koch, *Quantum Theory of the Optical and Electronic Properties of Semiconductors* (World Scientific, Singapore, 1990).
[62]A. L. Fetter and J. D. Walecka, *Quantum Theory of Many-Particle Systems* (McGraw-Hill, New York, 1971), Chap. 5.
[63]G. D. Mahan, *Many-Particle Physics* (Plenum, New York, 1986), p. 466.
[64]H. Haug and S. W. Koch, Phys. Rev. B **39**, 1887 (1989).
[65]C. Weber, C. Klingshirn, D. S. Chemla, D. A. B. Miller, J. E. Cunningham, and C. Ell, Phys. Rev. B **38**, 12 748 (1988).